Mutation in the Zebrafish *cct2* Gene Leads to Abnormalities of Cell Cycle and Cell Death in the Retina: A Model of *CCT2*-Related Leber Congenital Amaurosis

Yuriko Minegishi,* Naoki Nakaya, and Stanislav I. Tomarev

Section of Retinal Ganglion Cell Biology, Laboratory of Retinal Cell and Molecular Biology, National Eye Institute, National Institutes of Health, Bethesda, Maryland, United States

Correspondence: Stanislav I. Tomarev, National Eye Institute, 6 Center Drive, Building 6, Room 212, Bethesda, MD 20892, USA; tomarevs@nei.nih.gov.

*Current affiliation: Molecular and Cellular Biology Division, National Institute of Sensory Organs, Tokyo Medical Center National Hospital Organization, Tokyo, Japan.

Submitted: September 2, 2017
Accepted: January 15, 2018

Citation: Minegishi Y, Nakaya N, Tomarev SI. Mutation in the zebrafish *cct2* gene leads to abnormalities of cell cycle and cell death in the retina: a model of *CCT2*-related Leber congenital amaurosis. *Invest Ophthalmol Vis Sci*. 2018;59:995–1004. https://doi.org/10.1167/iovs.17-22919

Purpose. The compound heterozygous mutations in the β subunit of chaperonin containing TCP-1 (CCT), encoded by *CCT2*, lead to the Leber congenital amaurosis (LCA). In this study, a *cct2* mutant line of zebrafish was established to investigate the role of *CCT2* mutations in LCA in vertebrates.

Methods. A *cct2* mutant zebrafish line was produced using the CRISPR-Cas9 system. Changes in the eyes of developing wild-type and mutant larvae were monitored using microscopy, immunostaining, TUNEL, and EdU assays. Phenotypic rescue of mutant phenotype was investigated by injection of *CCT2* RNA into zebrafish embryos.

Results. The *cct2* mutation (*L394H-7del*) led to the synthesis of a mutated cctβ protein with the L394H replacement and deletion of 7 amino acid residues (positions 395–401). The homozygous *cct2-L394H-7del* mutant exhibited a small eye phenotype at 2 days post fertilization (dpf) and was embryonically lethal after 5 dpf. In homozygous *cct2-L394H-7del* mutants, the retinal ganglion cell differentiation was attenuated, retinal cell cycle was affected, and the neural retinal cell death was significantly increased at 2 dpf compared with wild-type. Injection of RNA encoding wild-type human CCTβ rescued the small eye phenotype, reduced retinal cell death, and restored the levels of CCTβ protein and the major client protein Gβ1 that were significantly reduced in the homozygous *cct2-L394H-7del* mutant compared with wild-type. These results indicate that *cct2* plays an essential role in retinal development by regulating the cell cycle.

Conclusions. The retinal pathology observed in the homozygous *cct2-L394H-7del* mutants resembles the retinal pathology of human LCA patients.

Keywords: Leber congenital amaurosis, zebrafish, retina, *CCT2*, CRISPR-Cas9

Leber congenital amaurosis (LCA) is an early onset genetic retinal disease that is one of the top causes of child blindness.[1–3] The manifestation of LCA is quite heterogeneous and it sometimes shares overlapping symptoms with other genetic retinal disorders. To date, mutations in approximately 20 genes have been reported as LCA-causative. These genes are involved in phototransduction, retinoid cycling, cellular maintenance, ciliary functions, guanine synthesis, and retinal development. Recently, the compound heterozygous mutations in the *CCT2* gene have been identified by whole exome sequencing analyses.[4] These mutations led to two substitutions (T400P and R516H) in the amino acid sequence of the encoded CCTβ protein resulting in reduced stability and chaperone activity of the mutated protein. The knock down of endogenous *Cct2* in the mouse 661W photoreceptor-derived cell line reduced the cell proliferation.[4] A mutation in the zebrafish *cct2* gene obtained as part of a large scale insertional mutagenesis has also been reported.[5] The insertional mutation in the *cct2* gene led to a small eye and head phenotype but detailed analysis of mutant phenotypes has not been performed.

Chaperonin containing T-complex protein-1 (CCT) is one of the eukaryotic chaperon systems classified into group II chaperonin.[6] Eight genes (*CCT1–8*) encode proteins comprising CCT (CCTα-CCTθ, respectively). These eight subunits interact with each other to form the hetero-octameric ring structure that further dimerizes via the equatorial domain.[7] The staggered ring structure yields a cavity to fold a nascent protein into proper three-dimensional structure by adenosine triphosphate (ATP) hydrolysis. Each CCT subunit has distinct properties and interacts with numerous cochaperons to facilitate folding of specific client proteins.

Besides *CCT2* mutations, mutations in other genes encoding CCT subunits have been identified in humans, animals, and yeast. A homozygous missense mutation in *CCT5* encoding CCTε protein has been identified in a patient with familial sensory neuropathy with spastic paraplegia. This mutation led to H147R substitution in the amino acid sequence. In Sprague-Dawley rats, the spontaneous homozygous missense mutation in the *Cct4* gene encoding CCTδ produced the mutilated foot (*mf*) phenotype. This mutation (*C450Y*) caused severe degeneration of the sensory ganglia and fibers resulting in ataxia, insensitivity to pain, ulceration of the feet, and resembled the sensory neuropathy in humans. Mutations in zebrafish *cct1, 3, 4, 5, 7* have been produced as a result of a large scale mutagenesis screen designed to identify genes involved in embryonic development.[5,8,9] These mutants, similar

to the *cct2* insertional mutant, exhibited head and eye hypoplasia although the exact molecular processes leading to the identified defects remain elusive. Trimethylpsoralen mutagenesis was used to produce the *cct3* frame-shifted truncated mutation in zebrafish that was named nontectal neuron (*ntn*). Zebrafish that carried this mutation in a homozygous state also had hypoplastic head and eyes.[9] Results obtained with *CCT* mutants suggest that the CCT subunits play an important role in neuronal development.

The patients with the compound heterozygous mutations in *CCT2* exhibited common LCA symptoms, such as early onset blindness, sunken eyes, photophobia, and oculodigital signs.[4] The fundus images and examination by optical coherence tomography revealed highly hypoplastic retina with decreased brightness of the neuronal fiber layer and attenuated blood vessels in the affected individuals, indicative of early developmental defects. The development of animal models carrying mutations in the *CCT2* gene is one possible approach to elucidate its molecular mechanisms in retinal development.

In this study, a zebrafish line carrying in-frame deletion mutation in the *cct2* gene was established using the CRISPR-Cas9 system. Analysis of the retinal phenotype of homozygous mutant indicated that *cct2* contributes to the retinal development through the cell cycle defects, leading to significant cell death in the developing neural retina and subsequently a smaller eye phenotype. Mutant zebrafish phenotype resembled the retinal pathology of human LCA patients.

Methods

Husbandry of Zebrafish

The TL strain of zebrafish (*Danio rerio*) was used in this study. Zebrafish were maintained as described.[10] Embryos were produced by natural mating. All experiments using animals were approved by the National Eye Institute Animal Use and Care Committee and were maintained in accordance with guidelines described in the ARVO Statement for the Use of Animals in Ophthalmic and Vision Research.

Genome Editing by CRISPR-Cas9 and the Selection of *cct2* Mutant Fish

The CRISPR-Cas9 system was used to target the region of zebrafish *cct2* gene corresponding to the LCA-causing *T400P* mutation. This region encodes alpha helix 14 (H14) in the cctβ protein, which is important for the closure of apical domain of CCTs under the client protein processing.[11,12] The Ex-Taq PCR kit was used for the amplification of the targeted region and the PCR products were purified by the PCR purification kit (QIAGEN, Germantown, MD, USA). The targeted region of adult parental TL strain was sequenced using the following primers: 5′-ACAGAGTTTTCTGGAGTCTCCATGGTT-3′ and 5′-TACCATCATCAGGGCTTTGGCGAA-3′. Guide RNA (gRNA) for the targeted region of *cct2* was designed using OPTIMIZED-CRISPR (in the public domain, http://crispr.mit.edu/) and ZiFiT Targeter (in the public domain, http://zifit.partners.org/ZiFiT/). Because of the polymorphism 4 bp upstream of the targeted codon (corresponds to position 400 in the amino acid sequence), two gRNAs were simultaneously used. Two pairs of primers were used to clone guide gRNA sequences into the BsaI site of the pDR274 vector (Addgene, Cambridge, MA, USA). First pair: 5′-TAGGTGCTGGCACAGACCGTCA-3′ and 5′-AAACT GACGGTCTGTGCCAGCA-3′; second pair: 5′-TAGGTGCTGGCG CAGACCGTCA-3′ and 5′-AAACTGACGGTCTGCGCCAGCA-3′. The gRNAs were prepared using the MAXIscript T7 In Vitro Transcript Kit (Thermo Fisher Scientific, Cincinnati, OH, USA) with subsequent precipitation of the reaction mixtures with lithium chloride and ethanol. Cas9 nuclease containing the nuclear localization signal (NLS) was purchased from New England Biolabs (Ipswich, MA, USA). The gRNA-Cas9 injection mix included two gRNAs (15 ng/μL each, total 30 ng/μL) and Cas9-NLS protein (5 pmol/μL). One- to two-cell stage zebrafish embryos were injected with 1 nL of the gRNA-Cas9 injection mixture. Eight injected fish were raised as founder fish and cross-mated to validate the germ line transmission to the F1 generation. The mutations were first examined by analyzing the trace patterns of direct sequencing reactions and then by sequencing of plasmid DNAs produced by TA-cloning using corresponding PCR products and the T-Vector pMD20 TA cloning kit (Takara Bio, Inc., Madison, WI, USA). The F2 generation was obtained by crossmating the F1 heterozygous males carrying a mutation with wild-type females. The primers 5′-TGAGGCGTGCACTATCGTCCTG-3′ and 5′-CTCCATATA CAGTGCGCGTCTCC-3′ were used for PCR genotyping of selected mutants. PCR products were analyzed using 2% agarose gels. Stemi DV4 (Carl Zeiss, Inc., Thornwood, NY, USA) stereoscope was used for macroscopic observations with subsequent measurements of the eye area using the ImageJ software (https://imagej.nih.gov; provided in the public domain by the National Institute of Health, Bethesda, MD, USA).

Immunohistochemistry, TUNEL, and EdU Assays

Zebrafish embryos were fixed with ice-cold 4% paraformaldehyde (PFA) in PBS overnight. Fixed samples were cryoprotected with 30% sucrose in PBS and embedded in the 1:2 mixture of 30% sucrose PBS and Tissue-Tek O.C.T. compound (Sakura Finetek, Torrance, CA, USA). Cryosections, 14-μm thick, were prepared and stored at –80°C. For immunostaining, sections were washed twice with PBS and then blocked with a casein blocker in PBS (Thermo Fisher Scientific) for 15 minutes at room temperature. Antibodies against zn-5 (1:100; Development Studies Hybridoma Bank, Iowa City, IO, USA), Phospho-Histone 3 (PH3; 1:1000; Merck Millipore, Burlington, MA, USA), and zpr-1 (1:200; Development Studies Hybridoma Bank) were used for immunostaining. Sections were incubated with primary antibodies in the blocking reagent (Thermo Fisher Scientific) at 4°C overnight, washed three times with PBS and then incubated with Alexafluor 488 or 594-labeled anti-rabbit or anti-mouse secondary antibodies (Thermo Fisher Scientific) for 45 minutes at room temperature. Nuclei were counterstained with Hoechst 33342. Sections were then washed three times with PBS and mounted using FluorSave Reagent (EMD Millipore, Billerica, MA, USA). A Zeiss LSM700 confocal microscope with a Zen software was used for imaging. Three normal or three mutant embryos and two to three sections per an individual embryo were used for each immunostaining. ClickIT plus TUNEL kit (Thermo Fisher Scientific) was used to analyze cell death as described by the manufacturer with a minor modification: the incubation of cryosections with proteinase K was reduced from 15 to 5 minutes. Five normal and eight mutant embryos were analyzed by TUNEL and two to three sections per an individual embryo were analyzed. The ClickIT plus EdU (Thermo Fisher Scientific) assay kit was used to detect the S-phase cells. The dechorionated embryos at 2 days post fertilization (dpf) were incubated with 3 mM EdU in E3 embryo medium (50 mM NaCl, 0.17 mM KCl, 0.33 mM $CaCl_2$, 0.33 mM $MgSO_4$) for 3 hours at 28°C, fixed in 4% PFA, cryopreserved as described above, and then processed according to the manufacturer's instructions. For double EdU and PH3 staining, specimens were blocked with BSA in PBS after Edu staining and immunostained with PH3 antibodies as described above. Five normal and five mutant embryos were

Investigative Ophthalmology & Visual Science

analyzed by EdU/PH3 double labeling and two to three sections per an individual embryo were analyzed.

Phenotypic Rescue of Mutant Phenotype by RNA Injection

The human wild-type *CCT2* and *T400P* mutant were cloned into the BamHI site of the pCS2+ vector. The pCS2+ plasmid of *CCT2* with *L394H-7del* mutation was obtained by using the Q5 Site-Directed Mutagenesis Kit (New England Biolabs). First, a 21-bp deletion was introduced into the plasmid and then one nucleotide was substituted to obtain the *H394L-7del* mutation in human *CCT2*. The mMESSAGE mMACHINE SP6 kit (Thermo Fisher Scientific) was used for the RNA synthesis according to the manufacturer's instructions. For the rescue analyses, 100 or 200 pg of mRNA for different CCTβ variants were injected into one- to two-cell stage embryos obtained as a result of F2 × F2 matings. Three independent cycles of egg production and RNA injections were performed using four males and four females. To score the small eye phenotype, embryos were aligned on a gel plate with a ruler and each eye was enclosed using a freehand selection tool and ImageJ.

Western Blot Analysis

Embryos were lysed in TNE buffer (50 mM Tris, 150 mM NaCl, 1 mM EDTA, 0.1% NP-40) with two pulses of sonication using Sonic Dismembrator (Thermo Fisher Scientific). The supernatant fractions were prepared by centrifugation at 20,000*g* at 4°C for 15 minutes. The equal amounts of lithium dodecyl sulfate sample buffer were added to lysate samples with subsequent denaturation at 95°C for 5 minutes. Denaturated samples were separated using the Bolt 8% Bis Tris Plus gel with 2-(*N*-morpholino) ethanesulfonic acid (MES) SDS running buffer. The iBlot2 system was used for polyvinylidene difluoride (PVDF) membrane transfer. The membranes were blocked with 10% blocking buffer (Thermo Fisher Scientific) in PBS-0.1% Tween 20 (PBS-T) for 10 minutes at room temperature. The antibodies used were: anti-CCTβ (1:500; Cell Signaling Technology, Danvers, MA, USA), anti-Gβ1 (1:1000; Abcam, Cambridge, MA, USA), anti-Hsc70 (1:1000; Santa Cruz Biotechnology, Santa Cruz, CA, USA), and anti-Actin (1:1000; Santa Cruz Biotechnology). Ponceau S staining of membranes after transfer was used for the normalization of protein loading. Amersham ECL antibodies conjugated with HRP (1:10,000; GE Healthcare, Pittsburgh, PA, USA) were used as secondary antibodies and the West Fento (Thermo Fisher Scientific) was used for detection. The developed images were captured by Amersham Imager 600 (GE Healthcare). The intensities of bands were quantified according to the manufacturer's instructions. All Western blotting experiments were repeated at least twice.

Statistical Analysis

All data were expressed as mean ± standard error (SE). Student's *t*-test was used for statistical analyses. χ^2 test was used to validate the deviation of Mendelian inheritance. *P* values < 0.05 were considered as statistically significant.

Results

Generation of a Zebrafish Line Carrying the In-Frame Deletion *L394H-7del* Mutation in *cct2*

The amino acid sequence of CCTβ is highly conserved across species. So, the identity of zebrafish and human sequences is 91% (Fig. 1A). The threonine codon corresponding to position 400 in the amino acid of zebrafish cctβ was chosen as a target for genome editing because previous data demonstrated that the compound heterozygous mutations of *T400P* and *R516H* in CCTβ led to LCA in humans.[4] There is a single *cct2* gene in the zebrafish genome and the CRISPR-Cas9 genome editing system was used to generate mutations. While a polymorphism A/G (position 1194 in the coding region of corresponding cDNA) was detected in the nucleotide sequence near the area of interest (positions 1198–1200 corresponding to threonine in position 400 in the amino acid sequence) by direct genome sequencing in the parental zebrafish of TL strain. Therefore, two gRNAs corresponding to polymorphic sequences were prepared and injected simultaneously into embryos to increase the genome editing efficiency (Fig. 1B). Eight independent founders were raised to adult stage, of which five were mosaic. Three of them contained different in-frame mutations and two had different frame-shifting mutations around the targeted protospacer adjacent motif (PAM) sequence as shown by genomic sequencing of DNA isolated from their tails. Two-month-old F1 fish were genotyped individually and one F1 fish containing a 21-bp deletion (corresponds to positions 395–401 in the amino acid sequence) and replacement of two nucleotides leading to the *L394H* replacement was identified (Fig. 1C). This line was named *cct2-L394H-7del* and selected for subsequent analysis because of the two main reasons: (1) there was no zebrafish line with in-frame mutation in *cct2*, and (2) it was easy to genotype this mutant to establish a novel zebrafish *cct2-L394H-7del* mutant line. Mating the F1 *cct2-L394H-7del* mutant with wild-type fish produced 31 F2 fish and they were genotyped at 3 months of age. Fourteen (45.2%) F2 fish were heterozygous for *cct2-L394H-7del* mutation indicating that this mutation is not lethal in the heterozygous state.

Characterization of *cct2-L394H-7del* Mutant Phenotype

F2 *cct2-L394H-7del* heterozygous fish were cross-mated to produce F3 homozygous mutants and investigate their eye phenotype. Five independent crosses using four females and four males were performed. Some embryos had smaller eyes compared with other embryos and these differences were clearly distinguishable within the F3 progeny at 2 dpf (Fig. 2A), becoming more pronounced at 3 dpf (Fig. 2B). At this stage, smaller eyes had a circular shape versus an elliptic to oval shape of the eyes in most embryos. In addition, *cct2-L394H-7del* homozygous fish had a smaller head size, bended body, and larger yolk sacs compared with wild-type fish (Fig. 2B). Difference in size and shape of homozygous *cct2-L394H-7del* mutants allowed their identification by macroscopic observation. Among 970 analyzed embryos, 25.3% had small eyes indicating a recessive Mendelian inheritance (see Table). The genotyping demonstrated that embryos with smaller and circular eyes were homozygous of the *cct2-L394H-7del* mutation (Fig. 2C). No homozygous *cct2-L394H-7del* mutant embryos were found among embryos having eyes of normal size and shape. The eye grew in size with progression of development in wild-type and heterozygous mutant embryos, while in the homozygous *cct2-L394H-7del* mutant eye did not grow after 2 dpf. As a result, the eye area in homozygous *cct2-L394H-7del* mutants was reduced by 23%, 47%, and 59% of normal eye area at 2, 3 and 5 dpf, respectively (Fig. 2E). The developmental defects disabled homozygous mutant larvae from swimming at 5 dpf (Fig. 2D). Most of them died after this stage. These data indicate that *cct2* plays an important role in zebrafish development including ocular development.

Investigative Ophthalmology & Visual Science

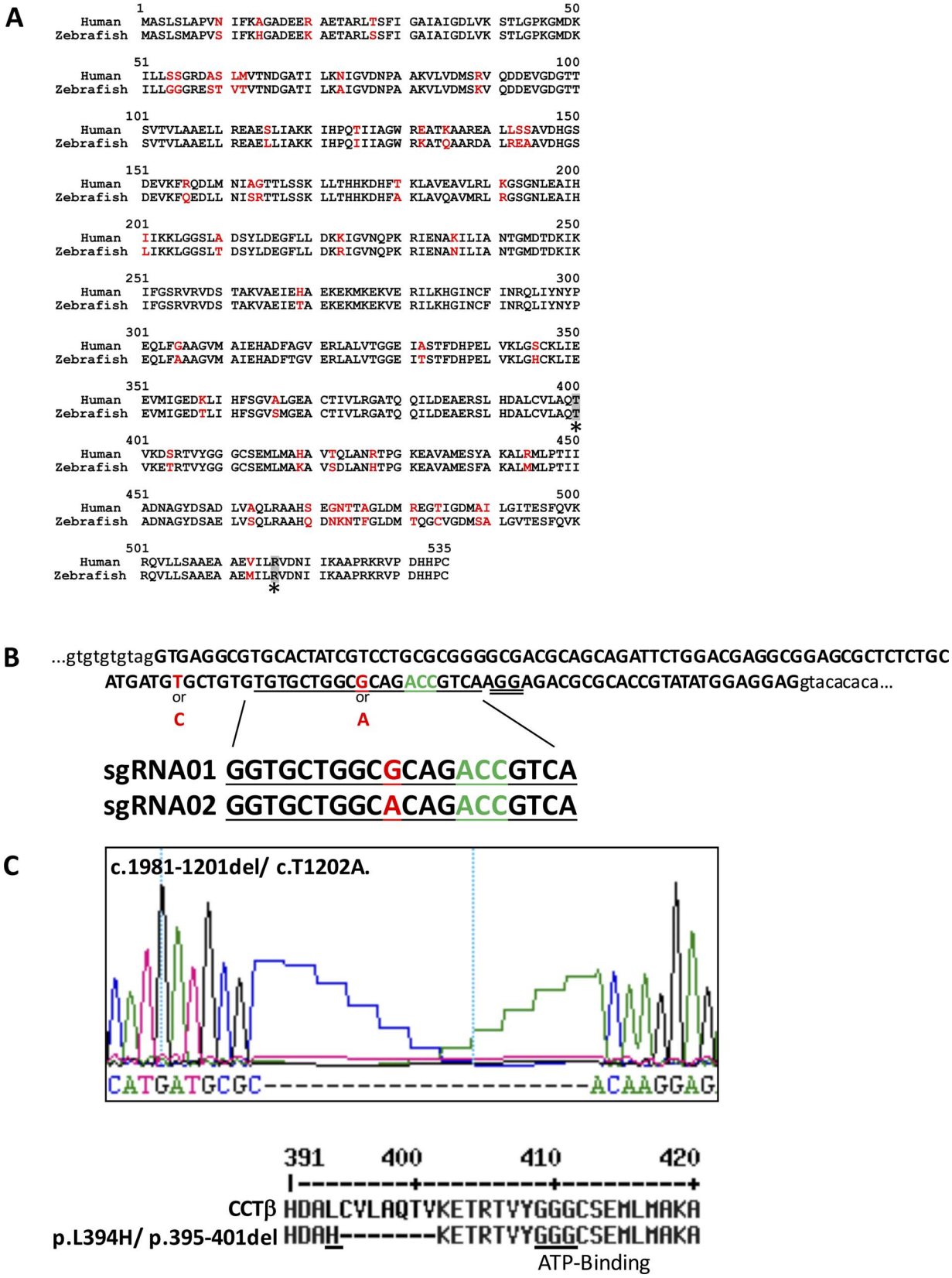

Figure 1. Strategy and summary of the genome editing for *cct2* by CRISPR-Cas9. (**A**) Comparison of human and zebrafish CCTβ amino acid sequences. The differing amino acid residues are shown in *red*. The position of LCA-associated mutations *T400* and *R516* are *shaded* and marked by *asterisks*. (**B**) The reference sequence of the targeted area of the zebrafish *cct2* gene in the TL strain. Exon 14 of *cct2* is depicted in capital letters. The intronic sequences surrounding this exon are depicted in lower case letters. The guide RNA sequences (*underlined* in the reference sequence) are shown below the reference sequence. T, the first 5′ nucleotide in the guide RNA sequences, was substituted by G for in vitro transcription using

Investigative Ophthalmology & Visual Science

T7 polymerase. The polymorphic positions are shown in *red*. The PAM sequence was *double underlined*. The codon corresponding to threonine 400 is shown in *green*. (**C**) Changes in the nucleotide and protein sequences of the *cct2-L394H-7del* mutant. *Upper panel* shows the nucleotide sequence. The lower panel shows translated wild-type and mutated proteins. The mutated *CCTβ* protein has the L394H substitution (*underlined*) and deletion of seven amino acids. The highly conserved ATP-binding motif is *underlined*.

Abnormalities of Retinal Development in the *cct2-L394H-7del* Homozygous Mutant

Because the *cct2-L394H-7del* homozygous mutant exhibited a smaller eye phenotype, histologic changes within the ocular tissues were investigated. At 2 dpf, the most dramatic changes were observed in the retinal ganglion cell (RGC) layer of mutant embryos. The RGC staining and the optic nerve thickness were reduced in the mutant compared with wild-type as shown by immunostaining with zn-5 antibodies that are specific for RGCs (Figs. 3A–B, white brackets). Lamination of the retina appeared to be less obvious in mutants compared with wild-type (Fig. 3A) and these defects became even more pronounced at 3 dpf (see Figs. 4D–I). At this developmental stage, many cells in the retina of wild-type larvae were positive for zpr-1, a cone photoreceptor marker. The number of zpr-1–positive was dramatically reduced in the *cct2-L394H-7del* homozygous mutant (Figs. 3C, 3D).

The smaller eye size and reduced zn-5 staining in homozygous *cct2-L394H-7del* mutants compared with wild-type suggested possible changes in cell proliferation. Therefore, we analyzed the cell cycle in wild-type and mutants by monitoring EdU incorporation (the S-phase indicator) and anti-PH3 immunostaining (M-phase marker). In wild-type embryos, the most of the EdU and PH3-positive cells were restricted to the ciliary marginal zone and the area of neuronal precursors

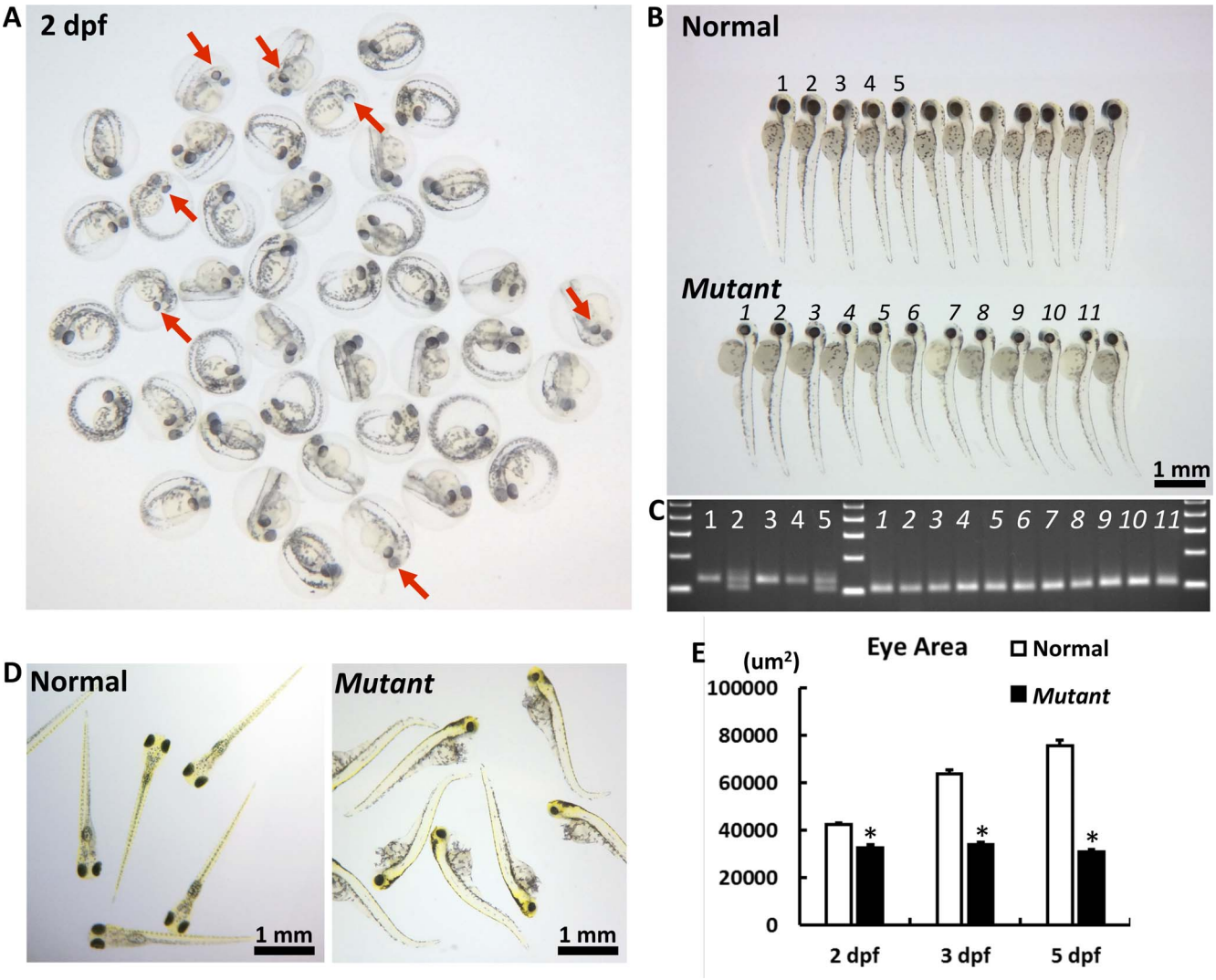

Figure 2. The macroscopic eye phenotype of the *cct2-L394H-7del* mutant. (**A**) The representative picture of F3 embryos from F2 cross mating at 2 dpf. At this stage, some embryos had smaller eyes with reduced pigmentation (marked by *red arrows*) compared with most embryos. (**B**) The representative picture of F3 embryos from F2 cross mating at 3 dpf. At this stage, the homozygous *cct2-L394H-7del* mutant embryos (*lower row*) were easily distinguished from wild-type and heterozygous *cct2-L394H-7del* embryos (*upper row*) by smaller size and circular shape of their eyes. The numbering (1–5 for normal eye and 1–11 for smaller eye larvae) is identical to the numbering in (**C**). (**C**) The genotyping of embryos labeled in (**B**) by PCR. The wild-type allele produces a 125-bp band, while the mutant allele produces a 101-bp band. (**D**) The representative picture of F3 embryos from F2 crossmating at 5 dpf. At this stage, wild-type and heterozygous larvae start to swim, while homozygous mutant larvae are not able to swim. (**E**) Comparison of the eye area between normal versus homozygous *cct2-L394H-7del* mutant embryos at 2, 3, and 5 dpf. $^*P < 0.05$.

Investigative Ophthalmology & Visual Science

Table. Rescue of a Small Eye Phenotype by *CCT2* RNA Injection

	Normal	Small Eye	Total	Small Eye, %	χ^2 Test
NIC	131	42	173	24.3	0.8263
Mock	87	23	110	20.9	0.3218
WT-100 pg	115	14	129	10.9	0.0002
WT-200 pg	168	13	181	7.2	3.10^{E-08}
TP-100 pg	90	33	123	26.8	0.6394
Delins-100 pg	109	30	139	21.6	0.2796

The incidence of small eye phenotype in the rescue study. NIC, *L394H-7del*, no injection control; Mock, mock injection of dye and TE buffer; WT-100 pg, 100 pg of wild-type *CCT2* RNA/embryo; WT-200 pg, 200 pg of wild-type *CCT2* RNA/embryo; TP-100 pg, 100 pg of *T400P* RNA/embryo; delins, 100 pg of *L394H-7del* RNA/embryo.

(Figs. 3F, 3G). The localization of PH3-positive cells in mutant retina was similar to that of the wild-type retina while EdU positive cells showed broader distributions in the neural retina compared with wild-type (Figs. 3H, 3I). The total number of EdU-positive S-phase cells was increased in mutant retinas compared with wild-type retinas (Fig. 3L), whereas the total number of PH3-positive M-phase cells was decreased (Fig. 3M). At the same time, there was no difference in the number of PH3 and EdU double positive cells between mutant and wild-type (Fig. 3N). These results indicated that the homozygous *cct2-L394H-7del* mutation reduced the population of proliferative M-phase cells, at least in part, as a result of the cell cycle defects during S-phase.

If the cell cycle defects during development in *cct2-L394H-7del* mutants is the only reason of a small eye phenotype, the mutant eye should increase in size over time but this increase should be less pronounced than in wild-type. However, the mutant eye did not grow between 2 and 5 dpf (Fig. 2E), despite the presence of proliferating cells in the mutant retina. This implied a probable involvement of retinal cell deaths in a small eye phenotype in the *cct2-L394H-7del* mutant. Indeed, the number of TUNEL-positive cells was very small in wild-type retinas (Fig. 3O), while the number of TUNEL-positive cells was dramatically increased in the mutant retina (0.6 ± 0.2 vs. 49.8 ± 8.0 TUNEL-positive cells in wild-type versus mutant, respectively; $n = 7$ for wild-type, $n = 9$ for mutant; $P = 0.0003$; Fig. 3P). The TUNEL-positive cells were also found in the brain optic tectum, the area of RGC axons projection (Fig. 3P). These results suggest that cell cycle defects in the developing retina of the homozygous *cct2-L394H-7del* mutants occurs through the elongation of S-phase accompanied by the retinal cell death.

Rescue of the Small Eye Phenotype of the Homozygous *cct2-L394H-7del* Mutant

To test whether the homozygous *cct2-L394H-7del* mutant phenotype could be rescued, we injected embryos with RNA encoding human wild-type CCTβ or its mutant variant leading to LCA in humans. We reasoned that CCTβ is a highly conserved protein and that human CCTβ protein may efficiently execute its functions in zebrafish. At 2 dpf, the level of cctβ protein was approximately five times lower in the homozygous *cct2-L394H-7del* mutants compared with wild-type embryos (Fig. 4B). The level of Gβ1, one of the client protein of CCTβ, was also decreased by approximately 30% in the mutant compared with wild-type embryos, while the level of Hsc70 was increased by approximately 90% in the mutant compared with wild-type (Fig. 4B). Injection of RNA encoding wild-type CCTβ or its *T400P* mutant led to synthesis of corresponding proteins at the level exceeding the level of CCTβ in uninjected embryos (Fig. 4B). At 3 dpf, the level of CCTβ protein was approximately 10 times lower and Gb1 was approximately 35% lower in the homozygous *cct2-L394H-7del* mutants compared with wild-type embryos (Fig. 4C). Expression of human CCTβ could not be detected in injected embryos at 3 dpf and at later developmental stages (data not shown).

The rescue effect was first evaluated by counting the embryos having normal and small eyes. Among F3 progeny produced by crossmating of F2 *cct2-L394H-7del* heterozygous fish (3 independent mating experiments, total 173 NIC embryos), 24.3% of uninjected embryos (NIC) exhibited small eye phenotype (Table). Embryos mock injected with TE buffer (110 injected embryos) exhibited 20.9% larvae with small eye phenotype. The frequencies of the small eye phenotype in both NIC and mock controls were not significantly deviated from the Mendelian inheritance as judged by χ^2 test. Injection of 100 pg/embryo (129 injected embryos) or 200 pg/embryo (181 injected embryos) with wild-type *CCT2* RNA reduced the incidence of the small eye phenotype to 10.9% and 7.2%, respectively (Table). The χ^2 tests revealed a significant deviation of the small eye phenotype frequencies after injection of wild-type *CCT2* RNA from the Mendelian ratio indicating that injection of wild-type *CCT2* RNA produces a rescue of the mutant phenotype in a dose-dependent manner. Injection of embryos with 100 pg/embryo of the LCA-causative *T400P* mutant RNA (123 injected embryos) or the *cct2-L394H-7del* mutant RNA (139 injected embryos) failed to rescue the mutant phenotype (26.8% and 21.6% small eye mutants, respectively). The frequency of the small eye phenotype was not changed following mutant RNA injections. Other details of potential changes in the retinal structure after injection on mutant RNA injection were not investigated at this moment.

Zn-5 and TUNEL staining were also used to analyze rescue effects of wild-type RNA injection. Retina from mock-injected homozygous *cct2-L394H-7del* mutants was highly fragile and disorganized (Figs. 4D, 4G) compared with the wild-type retina (Figs. 4F, 4I) at 3 dpf. The intensity of immunostaining with antibodies against anti–zn-5 was dramatically reduced in mutant larvae (Fig. 4D). The TUNEL staining revealed numerous apoptotic cells in the mutant retina (Fig. 4G). Remarkably, the ocular lens in the mutant larvae was well maintained and no TUNEL-positive cells were found throughout the analyses (Fig. 4G). The injection of wild-type *CCT2* RNA noticeably preserved the developing retina of the homozygous *cct2-L394H-7del* mutants, which had mostly normal retinal structure, pattern of zn-5 immunostaining and optic nerve axon bundles (Fig. 4E, 4H) similar to those of wild-type retina. Furthermore, the retinal cell death was remarkably reduced in the retina of rescued homozygous *cct2-L394H-7del* mutant. We concluded that the exogenous supply of wild-type *CCT2* RNA rescued the mutant phenotype in a dose-dependent manner.

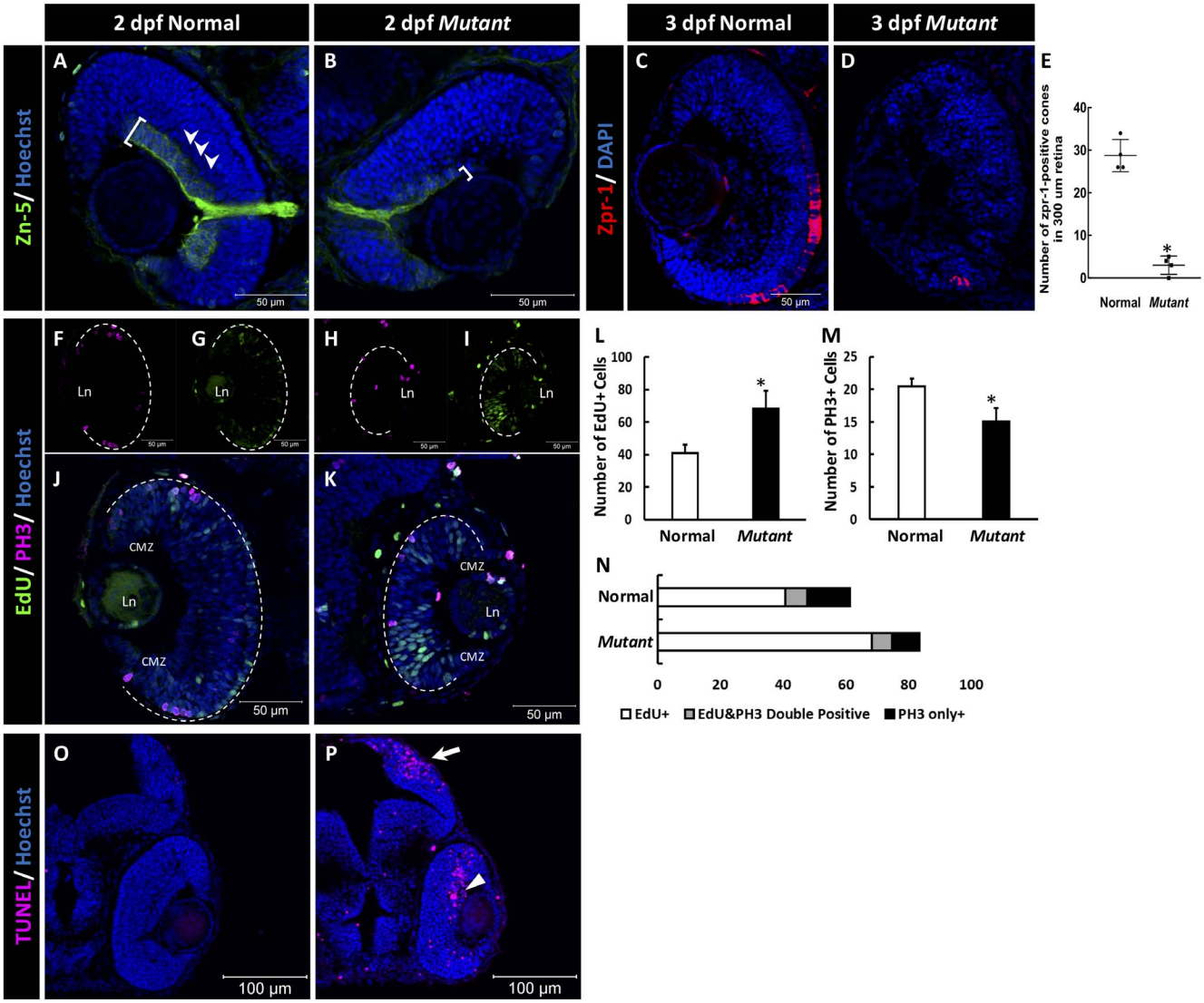

Figure 3. The retinal phenotype of the homozygous *cct2-L394H-7del* mutants at 2 pdf. (**A**, **B**) Staining of wild-type (**A**) and homozygous *cct2-L394H-7del* mutant (**B**) retinas with antibodies against Zn-5. Note a dramatic reduction of Zn-5 staining of the retinal ganglion cell layer (marked by a *white bracket*) and thinner optic nerve in *cct2-L394H-7del* mutant compared with wild-type. The lamination of the neural retina was more pronounced in wild-type embryos than in mutants. (**C**, **D**) The cone photoreceptor was underdeveloped in the homozygous *cct2-L394H-7del* mutants at 3 dpf. Staining of wild-type (**C**) and homozygous *cct2-L394H-7del* mutant (**D**) retinas with antibodies against zpr-1. (**E**) Quantification of zpr-1–positive cells in wild-type and homozygous *cct2-L394H-7del* mutant retinas ($n = 4$). (**F**–**I**) The distribution of PH3-positive and EdU-positive cells in the retina. In wild-type embryos, PH3-positive cells (**F**) and most of EdU-positive cells (**G**) were found in the ciliary marginal zone and the area of neuronal precursors localization. In the retina of homozygous *cct2-L394H-7del* mutants, PH3-positive cells were found in the ciliary marginal zone, area of neuronal precursors localization and lens epithelium (**H**). EdU-positive cells were found through the neural retina, in the ciliary marginal zone and lens epithelium (**I**). The *white dashed lines* indicate the eyecup boundaries. (**J**–**K**) Merged images of EdU and PH3 staining of the retina of wild-type (**J**) and homozygous *cct2-L394H-7del* mutant (**K**). (**L**–**N**) Quantification of EdU-positive, PH3-positive, and EdU/PH3-double positive cells in wild-type and homozygous *cct2-L394H-7del* mutant retinas ($n = 10$). (**O**, **P**) TUNEL staining of wild-type (**O**) and mutant (**P**) retinas. *Arrow* marks the optic tectum, the area of retinal ganglion cell axon projection; *arrowhead* marks TUNEL-positive cells in the neural retina. CMZ, ciliary marginal zone; Ln, lens. *Scale bars*: 50 μm. $^*P < 0.05$.

Discussion

In this study, we describe a novel zebrafish mutant line, *cct2-L394H-7del* produced by genome editing. This line contained a deletion of seven amino acids and one amino acid substitution in the alpha helix 14 of the CCTβ subunit. The homozygous *cct2-L394H-7del* mutation led to a small eye phenotype accompanied by changes in retinal morphology, a cell cycle defects through the elongation of S-phase and simultaneous cell death in the developing retina. The incidence of small eye phenotype was significantly reduced by injection of wild-type but not mutant *CCT2* RNA. The retina of rescued eyes had retinal morphology and pattern of zn-5 staining that were similar to those of wild-type embryos at 2 dpf. The phenotype observed in the homozygous *cct2-L394H-7del* mutant was more severe than in *CCT2*-LCA patients. Human patients carry two compound heterozygous mutations in *CCT2*, *T400P* and *R516H*. The level of the CCTβ protein is reduced almost 2-fold in LCA patient-derived T cells and induced pluripotent stem cells as compared with nonaffected patients. The *T400P* mutant is highly unstable and chaperoned by HSP90 that leads to rapid intracellular degradation. The *R516H* mutant protein

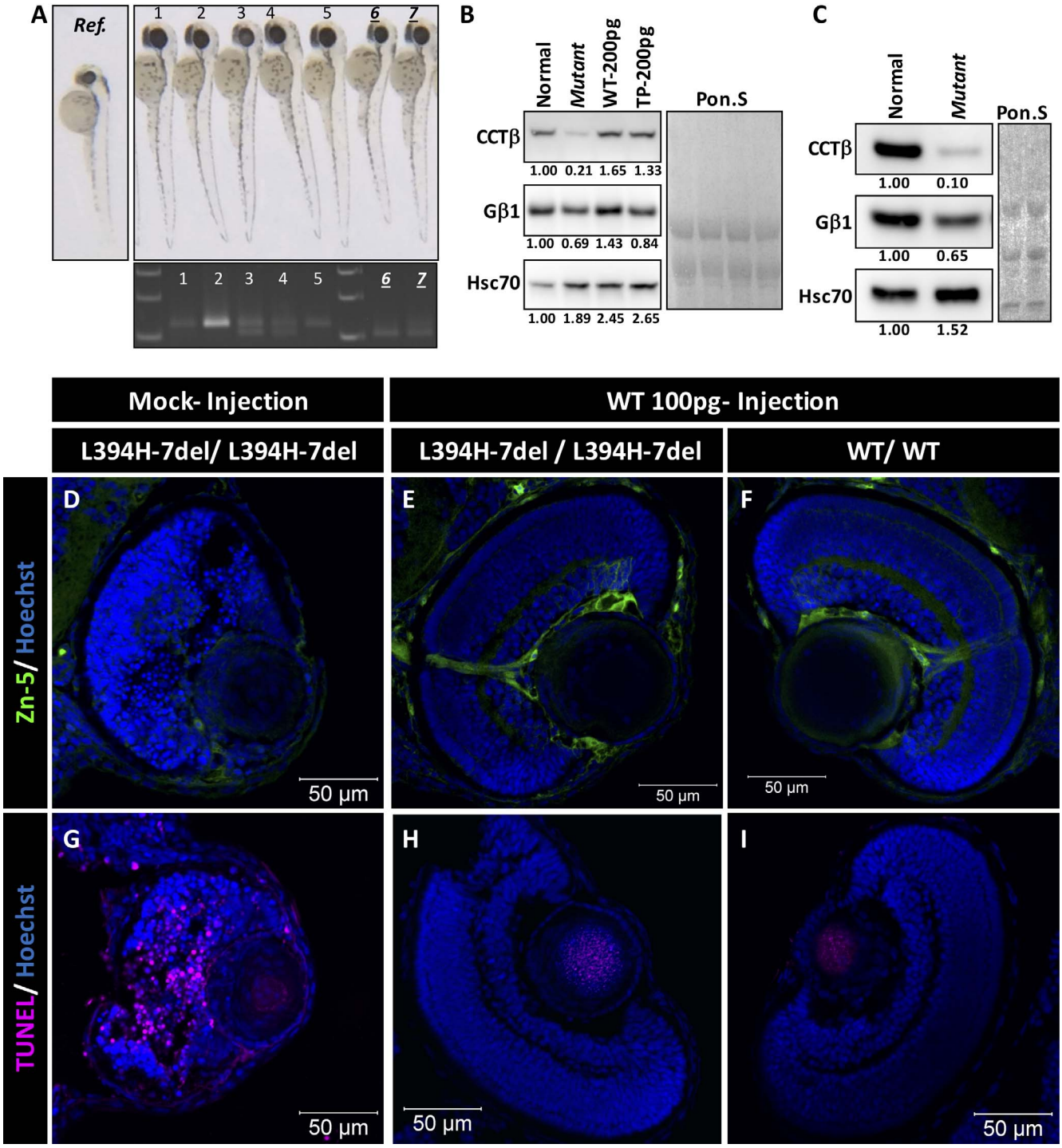

Figure 4. Rescue of a small eye phenotype by *CCT2* RNA injection. (**A**) Representative pictures of 2 dpf embryos after injection of wild-type human *CCT2* RNA (100 pg). Genotyping of injected embryos is shown *below*. Ref. panel shows uninjected *cct2-L394H-7del* mutant. (**B**) Western blot analysis of indicated proteins in 2-dpf embryos after injection of RNA encoding wild-type or LCA-causing T400P CCTβ. Normal and mutant lines correspond to uninjected control and mutant larvae. *Numbers* below each lane indicate changes in the protein level relatively to uninjected normal larvae after normalization using Poncer S (Pon. S) staining. Two independent sets of embryos were analyzed. (**C**) Western blot analysis of indicated proteins in 3-dpf embryos. Three independent sets of embryos were analyzed. (**D–E**) The zn-5 staining of homozygous 3-dpf *cct2-L394H-7del* mutant eye section after mocked (**D**) or wild-type *CCT2* RNA (**E**) injection. (**F**) The zn-5 staining of 3-dpf wild-type eye section after wild-type *CCT2* RNA injection. Size-rescued mutant retinas demonstrated zn-5 staining and lamination comparable to those of wild-type retina. (**G–I**) The TUNEL staining of the eye sections as in (**D–F**). Note the absence of TUNEL-positive cells in the size-rescued mutant retina.

is more stable than the *T400P* mutant but the *R516H* mutant is functionally compromised by is lower ability to interact with CCT.[4] The level of cctβ protein in the homozygous of *L394H-7del* mutant zebrafish is reduced almost 5-fold as compared with wild-type embryos at 2 dpf (Fig. 4B). We believe that this is one of the reasons of more severe phenotype in this zebrafish mutant as compared with the compound heterozygous mutations in human patients. The production and analysis

Investigative Ophthalmology & Visual Science

of T400P and R516H knock-in models of *CCT2*-related LCA may further clarify the impact of compound heterozygosity.

LCA patients carrying compound heterozygous *CCT2* mutations had highly hypoplastic retina exhibiting a reduced brightness of the neuronal fiber layer and attenuated blood vessels.[4] The development of retinal vasculature is a stepwise event that is designated primarily by the RGC development.[13] RGCs express PDGF-AA and axons of RGCs induce the proliferation of astrocytes expressing PDGF receptor α (PDGFRα), stimulating their migration into the retina along RGC axons.[14–17] The migrated astrocytes establish an astrocyte template on the surface of retina. The astrocytes express VEGF that enables the endothelial cells to proliferate and migrate into the retina along with the astrocyte templates.[13,17–19] Therefore, the RGC-deficiency attenuates retinal vasculature in RGC-deficient mouse models such as *brn3b*$^{Z\text{-}dta/+}$; *six3-cre* and *Math5*$^{-/-}$.[17,20,21] This indicates that the normal RGC development is essential for subsequent retinal development. Although detailed analysis of *cct2* expression in zebrafish has not been performed yet, available data indicate that the *cct2* mRNA is highly abundant in the head region including the eyes of developing zebrafish (https://zfin.org/ZDB-FIG-050630-10430). In mice, expression of *Cct2* was detected in developing RGCs during embryonic development (in the public domain, http://www.eurexpress.org/ee/intro.html). In adult mouse retina, CCTβ protein was preferentially localized in RGCs and photoreceptors.[4] Because the homozygous *cct2-L394H-7del* mutation exhibited the RGC defects, *CCT2* may as well contribute to RGC development in human. The disease manifestation of highly hypoplastic retina in the *CCT2*-LCA patient detectable already at 6 months of age may originates from the defects in RGC development in combination with the photoreceptor degeneration. Abnormal RGC development should be a key event that can lead to congenital retinal diseases with hypoplastic retina. We anticipate that additional information supporting this idea will be obtained using the T400P and R516H knock-in animal models.

In the retina of *cct2-L394H-7del* mutant fish, the cell cycle defects attenuated RGCs and cell death were the main phenotypic manifestations. It has been previously reported that a mutation in the yeast *cct2* gene led to the elongation of cell cycle.[22] The corresponding yeast mutant exhibited the 4N DNA content and demonstrated an increased cell size due to pseudo diploid phenotype.[22] Similarly, patient-derived induced pluripotent stem (iPS) cells carrying *T400P* and *R516H* compound heterozygous mutations have been reported to be less proliferative compared with the parental iPS cells.[4] Our data together with published data demonstrate that *CCT2* has a fundamental role in cell cycle maintenance.

Currently, it is not clear how the cell cycle elongation is connected to the cell death in the neural retina of the homozygous *cct2-L394H-7del* mutants. One possibility is that the cell cycle defects are associated with disorganization of cytoskeleton chaperoned by CCTβ that may lead to cell death. It has been reported that suppression of CCT functions by neutralizing antibody delays S-phase progression and disorganizes the cytoskeleton in mammalian cells[23] while the treatment of those cells with antibody against Hsp 27 affects actin stability and induces apoptosis in retinal neurons.[24] Recently, the tumorigenic association with upregulated CCT expression and the inducible apoptosis by blockade of β-tubulin/ CCTβ complex in drug-resistant tumors have been also reported.[25,26] CCT chaperonin provides stability of cytoskeleton that may play a role in cell viability. Another possibility is that cell cycle elongation may lead to desynchronization of development within the population of cells. In zebrafish, it has been reported that all cells in the eye primordium are proliferative until 28 hpf. At the same time, the cell cycle progression was slowed down between 16 and 24 hpf to synchronize the cell cycle within local populations.[27] Differentiation of RGCs and formation of pigmented epithelium occur between 27 and 36 hpf. The synchronization of cell cycle by its elongation before the neurogenesis has been also reported in developing retina in the vicinity of the morphogenetic furrow in the *Drosophila*.[28] The genetically desynchronized cell cycle resulted in the abnormal patterning of the ommatidium.[29] Lastly, the cell cycle elongation may affect the spaciotemporal axon guidance of RGC axons resulting in the deprivation of the neurotrophic factors important for RGC viability, such as brain derived neurotrophic factor (BDNF).[30] The significant increase of EdU-positive cells in the neural retina of the homozygous *cct2-L394H-7del* mutants implies the distortion of the synchrony of retinogenesis that attenuated the RGC differentiation and induced the cell deaths.

CCT chaperonin has multiple roles in adult organisms as well. It is involved in neural homeostasis by clearance of the pathogenic aggregations. The apical domain of CCTβ mitigates the neurotoxic Huntingtin aggregation through the chaperon function suggesting possible therapeutic application of CCT in neurodegenerative disorders.[31] More recently, the CCT has been reported to promote the degradation of neurotoxic protein aggregation via autophagy.[32] The crystallography and high resolution cryo-EM unveiled the mechanisms of CCT action.[11] Based on the nature of CCT hetero-octameric feature of intraring alignment and functional polarity by ATP-binding affinity, the CCTδ is predicted to have the most severe impact followed by CCTβ and CCTε. It is still not clear how the localization of mutations within CCT subunits or the substrate specificity of each subunit defines disease specificity. Two mutations in CCTβ that we described (*T400P* and *L394H-7del*) are in helix 14 and evoke retinal phenotype. The zebrafish *cct3* insertion mutant exhibited the retinal phenotype similar to that of *cct2-L394H-7del* mutant.[33] It would be very interesting to produce *CCT2* mutants with mutations identical to the *C450Y* mutation in *CCT4* or the *H147R* mutation in *CCT5* to test whether they will evoke the sensory neuropathy, LCA, or any other phenotype.

Mutations in different CCT subunits lead to distinct phenotypes in mammals. Mutant fish with viral insertions in *cct1*, *2*, *3*, *4*, *5*, or *7* have been reported to have small eye and head phenotype but detailed analysis of mutant phenotypes has not been performed.[5,8,9] Detailed analysis of these and other *cct* mutants could be useful for better understanding of the functions of individual subunits in the retina and other tissues.

Acknowledgments

The authors thank Benjamin Feldman, PhD, and Reiko Toyama, PhD, (National Institute of Child Health and Human Development) for valuable discussions on CRISPR-Cas9 in zebrafish, Ben Mead, PhD, for critical reading of the manuscript, and Anna Larson and Tyler Fayard (National Eye Institute) for the excellent care and husbandry of zebrafish.

Supported by the Intramural Research Program of the National Eye Institute and fellowship from JSPS Research Fellow of Japanese Biomedical and Behavioral Researchers at the National Institutes of Health (YM; Bethesda, MD, USA).

Disclosure: **Y. Minegishi**, None; **N. Nakaya**, None; **S.I. Tomarev**, None

References

1. Chacon-Camacho OF, Zenteno JC. Review and update on the molecular basis of Leber congenital amaurosis. *World J Clin Cases*. 2015;3:112–124.

2. Khan AO, Al-Mesfer S, Al-Turkmani S, Bergmann C, Bolz HJ. Genetic analysis of strictly defined leber congenital amaurosis with (and without) neurodevelopmental delay. *Br J Ophthalmol*. 2014;98:1724–1728.
3. Koenekoop RK. An overview of leber congenital amaurosis: a model to understand human retinal development. *Surv Ophthalmol*. 2004;49:379–398.
4. Minegishi Y, Sheng X, Yoshitake K, et al. Cct2 mutations evoke Leber congenital amaurosis due to chaperone complex instability. *Sci Rep*. 2016;6:33742.
5. Golling G, Amsterdam A, Sun Z, et al. Insertional mutagenesis in zebrafish rapidly identifies genes essential for early vertebrate development. *Nature Genet*. 2002;31:135–140.
6. Lopez T, Dalton K, Frydman J. The mechanism and function of group ii chaperonins. *J Mol Biol*. 2015;427:2919–2930.
7. Ditzel L, Lowe J, Stock D, et al. Crystal structure of the thermosome, the archaeal chaperonin and homolog of cct. *Cell*. 1998;93:125–138.
8. Amsterdam A, Burgess S, Golling G, et al. A large-scale insertional mutagenesis screen in zebrafish. *Genes Dev*. 1999; 13:2713–2724.
9. Amsterdam A, Nissen RM, Sun Z, Swindell EC, Farrington S, Hopkins N. Identification of 315 genes essential for early zebrafish development. *Proc Natl Acad Sci U S A*. 2004;101: 12792–12797.
10. Westerfield M. *The Zebrafish Book. A Guide for the Laboratory Use of Zebrafish (danio rerio)*. Eugene: University of Oregon Press; 2007.
11. Skjaerven L, Cuellar J, Martinez A, Valpuesta JM. Dynamics, flexibility, and allostery in molecular chaperonins. *FEBS Lett*. 2015;589:2522–2532.
12. Seo S, Baye LM, Schulz NP, et al. Bbs6, bbs10, and bbs12 form a complex with cct/tric family chaperonins and mediate bbsome assembly. *Proc Natl Acad Sci U S A*. 2010;107:1488–1493.
13. Fruttiger M. Development of the retinal vasculature. *Angiogenesis*. 2007;10:77–88.
14. Dakubo GD, Beug ST, Mazerolle CJ, Thurig S, Wang Y, Wallace VA. Control of glial precursor cell development in the mouse optic nerve by sonic hedgehog from retinal ganglion cells. *Brain Res*. 2008;1228:27–42.
15. Burne JF, Raff MC. Retinal ganglion cell axons drive the proliferation of astrocytes in the developing rodent optic nerve. *Neuron*. 1997;18:223–230.
16. Fruttiger M, Calver AR, Kruger WH, et al. Pdgf mediates a neuron-astrocyte interaction in the developing retina. *Neuron*. 1996;17:1117–1131.
17. O'Sullivan ML, Punal VM, Kerstein PC, et al. Astrocytes follow ganglion cell axons to establish an angiogenic template during retinal development. *Glia*. 2017;65:1697–1716.
18. Nakamura-Ishizu A, Kurihara T, Okuno Y, et al. The formation of an angiogenic astrocyte template is regulated by the neuroretina in a hif-1-dependent manner. *Dev Biol*. 2012;363: 106–114.
19. Dorrell MI, Friedlander M. Mechanisms of endothelial cell guidance and vascular patterning in the developing mouse retina. *Prog Retinal Eye Res*. 2006;25:277–295.
20. Sapieha P, Sirinyan M, Hamel D, et al. The succinate receptor gpr91 in neurons has a major role in retinal angiogenesis. *Nature Med*. 2008;14:1067–1076.
21. Edwards MM, McLeod DS, Li R, et al. The deletion of math5 disrupts retinal blood vessel and glial development in mice. *Exp Eye Res*. 2012;96:147–156.
22. Amit M, Weisberg SJ, Nadler-Holly M, et al. Equivalent mutations in the eight subunits of the chaperonin cct produce dramatically different cellular and gene expression phenotypes. *J Mol Biol*. 2010;401:532–543.
23. Grantham J, Brackley KI, Willison KR. Substantial cct activity is required for cell cycle progression and cytoskeletal organization in mammalian cells. *Exp Cell Res*. 2006;312: 2309–2324.
24. Tezel G, Wax MB. The mechanisms of hsp27 antibody-mediated apoptosis in retinal neuronal cells. *J Neurosci*. 2000;20:3552–3562.
25. Lin YF, Lee YF, Liang PH. Targeting beta-tubulin:Cct-beta complexes incurs hsp90- and vcp-related protein degradation and induces er stress-associated apoptosis by triggering capacitative ca2+ entry, mitochondrial perturbation and caspase overactivation. *Cell Death Dis*. 2012;3:e434.
26. Lin YF, Tsai WP, Liu HG, Liang PH. Intracellular beta-tubulin/chaperonin containing tcp1-beta complex serves as a novel chemotherapeutic target against drug-resistant tumors. *Cancer Res*. 2009;69:6879–6888.
27. Li Z, Hu M, Ochocinska MJ, Joseph NM, Easter SS Jr. Modulation of cell proliferation in the embryonic retina of zebrafish (danio rerio). *Dev Dyn*. 2000;219:391–401.
28. Thomas BJ, Zipursky SL. Early pattern formation in the developing drosophila eye. *Trends Cell Biol*. 1994;4:389–394.
29. Penton A, Selleck SB, Hoffmann FM. Regulation of cell cycle synchronization by decapentaplegic during drosophila eye development. *Science*. 1997;275:203–206.
30. Isenmann S, Kretz A, Cellerino A. Molecular determinants of retinal ganglion cell development, survival, and regeneration. *Prog Retin Eye Res*. 2003;22:483–543.
31. Sontag EM, Joachimiak LA, Tan Z, et al. Exogenous delivery of chaperonin subunit fragment apicct1 modulates mutant huntingtin cellular phenotypes. *Proc Natl Acad Sci U S A*. 2013;110:3077–3082.
32. Pavel M, Imarisio S, Menzies FM, et al. Cct complex restricts neuropathogenic protein aggregation via autophagy. *Nat Commun*. 2016;7:13821.
33. Matsuda N, Mishina M. Identification of chaperonin cct gamma subunit as a determinant of retinotectal development by whole-genome subtraction cloning from zebrafish no tectal neuron mutant. *Develop*. 2004;131:1913–1925.

Investigative Ophthalmology & Visual Science